Bažant, Z.P. (2000). "Scaling laws for brittle failure of sea ice." *Preprints, IUTAM Symp. on Scaling Laws in Ice Mechanics* (Univ. of Alaska, Fairbanks, June), J.P. Dempsey, H.H. Shen and L.H. Shapiro, eds. Paper No. 3, pp. 1–23.

IUTAM

SCALING LAWS IN ICE MECHANICS AND ICE DYNAMICS

UNIVERSITY OF ALASKA FAIRBANKS
JUNE 13-16, 2000

FAIRBANKS

Sponsored by
BP AMOCO, IARC, IUTAM, MMS, NSF, USAR, ONR

Organized and Chaired by
J.P. Dempsey, H.H. Shen and L.H. Shapiro

SCALING LAWS FOR BRITTLE FAILURE OF SEA ICE

ZDENĚK P. BAŽANT

Walter P. Murphy Professor of Civil Engrg. and Materials Science
Northwestern University, Evanston, Illinois 60208, USA
z-bazant@northwestern.edu

Abstract. *Based on the premise that large-scale failure of sea ice is governed by fracture mechanics, recently validated by Dempsey's in-situ tests, the paper*[1] *presents simplified analytical solutions for (1) the load capacity of floating ice plate subjected to vertical load and (2) the horizontal force exerted by an ice plated moving against a fixed structure. The solutions reveal size effects of ice thickness, structure diameter and, in the case of a finite floe, the floe size. For vertical loading, the results agree with previous sophisticated numerical fracture simulations. The results contrast with the predictions of material strength or plasticity theories, which exhibit no size effect on the nominal strength of structure. The results on size effect are supported by recent numerical simulations and comparisons with field observations.*

1 Introduction

Because small scale laboratory tests of sea ice exhibit hardly any notch sensitivity and do not exhibit fracture mechanics behavior, many studies from early to recent times have treated sea ice failure according to either plasticity or elasticity theory with a strength limit (Bernstein 1929, Nevel 1958, Kerr, 1975, 1996; Sodhi 1995a,b, 1998). When size effect was observed in tests (e.g., Butiagin 1966), it was attributed to randomness of material strength as captured by Weibull (1939) theory (reviewed by Kittl and Diaz, 1988, and Bažant and Planas, 1998, and based on an idea of Mariotte, 1686, and extreme value statistics developed by Peirce, 1926, and Fisher and Tippett, 1928). However, such an explanation of size effect is dubious because the maximum load is not reached at the initiation of fracture but only after large stable crack growth (e.g. Bažant and Planas 1998). Rather, the explanation must be sought in fracture mechanics.

Many studies documented the brittlebess of ice (e.g., Weeks and Mellor 1984, Weeks and Assur 1972). Various recent experiments (Dempsey 1991, DeFranco and Dempsey 1994, DeFranco, Wei and Dempsey 1991), especially Dempsey's in-situ tests of record-size specimens (Dempsey et al. 1999a,b; Mulmule et al. 1995; Dempsey et al. 1995), indicate that sea ice does follow fracture mechanics and on scales larger than about 10 m is very well described by linear elastic fracture mechanics (LEFM). Consequently, the size effects of fracture mechanics (Bažant 1984, 1993, 1997a,b, 1999; Bažant and Planas 1998; Bažant and Chen 1997) must get manifested, and should be strong especially in all the problems in which large

[1]Partial financial support under grant N00014-91-J-1109 from the Office of Naval Research and grant CMS-9713944 from the National Science Foundation, both to Northwestern University, is gratefully acknowledged.

cracks grow stably prior to reaching the maximum load. This includes two fundamental problems: (1) vertical load capacity of floating ice plate (penetration fracture), and (2) the maximum horizontal force exerted on a fixed structure by a moving ice plate. The latter problems has been analyzed by fracture mechanics at various levels of sophistication in several recent works (Bažant and Li 1994, Li and Bažant 1994, Bažant and Kim 1998, Dempsey et al. 1995). Some of these studies, particularly Bažant and Kim (1998), confirm that indeed a strong size effect ought to be present. Fracture analysis of another problem, namely the large-scale thermal bending fracture of floating ice (Bažant 1992a,b), also indicated a strong size effect.

The purpose of the present study is to analyze the size effects by a simplified analytical approach leading to explicit formulae for the nominal strength of the ice plate as a function of the size and geometry. Such an approach helps intuitive understanding, clarifies the failure mechanism, facilitates optimization of engineering design, elucidates the role of energy release as the main source of size effect, and readily reveals how material and geometry parameters control the size effect.

2 Vertical Load Capacity and Penetration

2.1 Review or Previous Numerical Fracture Analysis of Size Effect

Before embarking on an analytical approach, it may be useful to review recent detailed numerical simulation of fracture of floating ice caused by a vertical load (Bažant and Kim 1998). The fracture pattern (for the case of 6 radial cracks) is shown in Fig. 1a. The radial cracks at maximum load penetrate through only a part of ice thickness (Dempsey et al. 1995, Bažant and Li 1995); Fig,. 1b,c. The radius of each crack is divided by nodes into vertical strips in each of which the crack growth obeys Rice and Levy's (1972) 'nonlinear line-spring' model relating the normal force N and bending moment M in the cracked cross section to the relative displacement Δ and rotation θ (Fig. 1b).

The analysis is based on a simplified version of the cohesive crack model in which the vertical crack growth in each vertical strip is initiated according to a strength criterion. The cross section behavior is considered elastic-plastic until the yield envelope in the (N, M) plane is crossed by the point (N, M) corresponding to fracture mechanics. For ease of calculations, a non-associated plastic flow rule corresponding to the vector $(\mathrm{d}\Delta, \mathrm{d}\theta)$ based on fracture mechanics is assumed.

The following ice characteristics have been used in calculations: tensile strength $f'_t = 0.2$ MPa, fracture toughness $K_c = 0.1$ MPa $\sqrt{\mathrm{m}}$, Poisson ratio $\nu = 0.29$, and Young' modulus $E = 1.0$ GPa, with the corresponding values: fracture energy $G_f = K_c^2/E = 10$ J/m^2, and Irwin's fracture characteristic length $l_0 = (K_c/f'_t)^2$ = 0.25 m (this value happens to be about the same as for concrete).

Fig. 1e displays, with a strongly exaggerated vertical scale, the calculated crack profiles at subsequent loading stages. Fig. 1f shows the numerically calculated plot of the radial crack length a versus the ice thickness h ('fracture length' means the radial length of open crack, and 'plastic length' the radial length up to the tip of plastic zone). This plot reveals that, except for very thin ice, the radial crack length

$$a \approx c_h h \tag{1}$$

where $c_h \approx 24$ for the typical ice properties assumed.

The size effect is understood as the dependence of the nominal strength σ_N on structure size, which is in this case represented by ice thickness h. The nominal strength, which is not a material state variable but a parameter of the applied

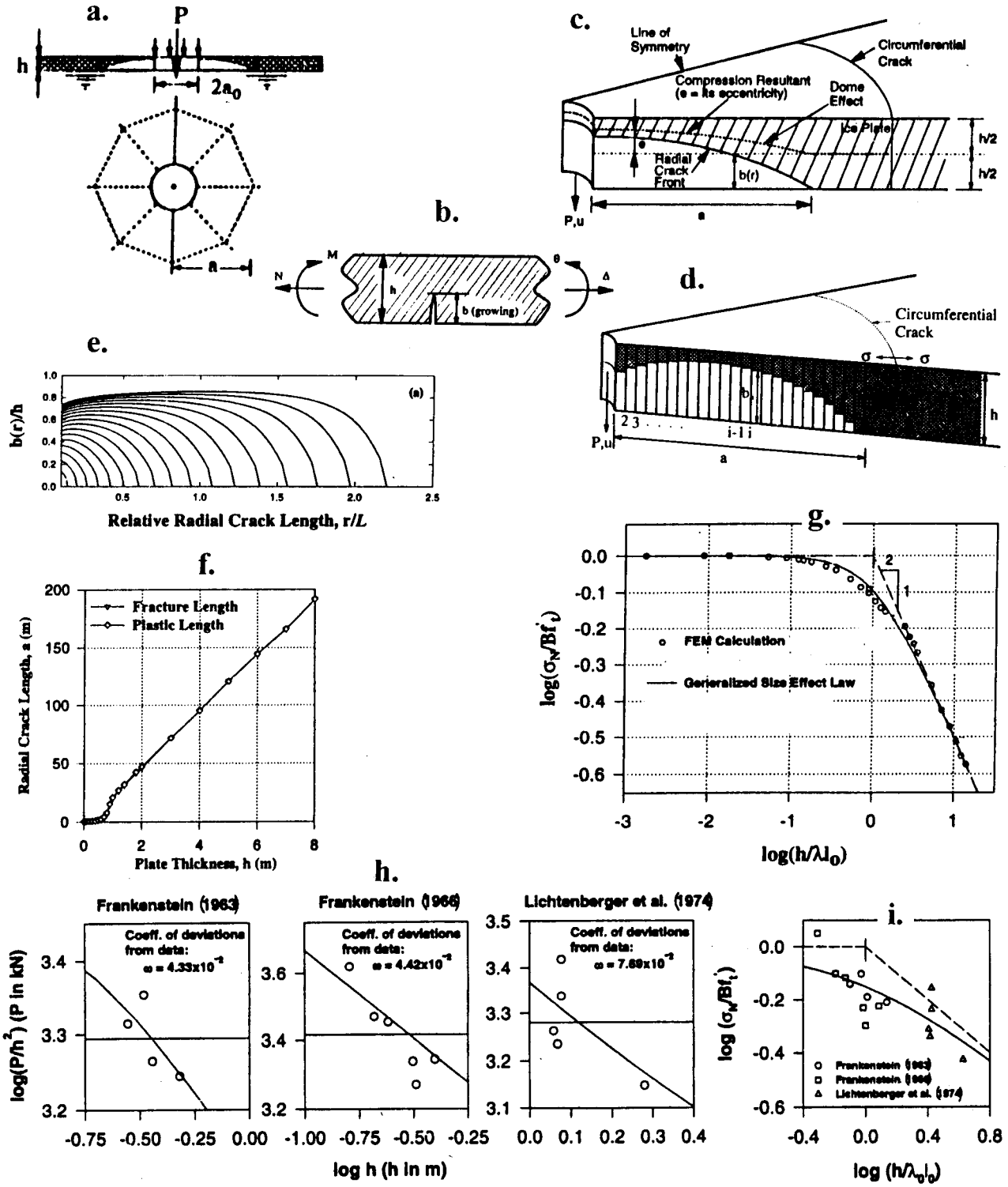

Figure 1: Vertical penetration fracture problem analyzed by Bažant and Kim (1998), main numerical results, and comparison with field tests of Frankenstein (1963,1966) and Lichtenberger (1974).

vertical load P, may be defined for the vertical penetration problem as

$$\sigma_N = P/h^2 \tag{2}$$

The data points in Fig. 1g show, in logarithmic scales, the numerically obtained size effect plot of the normalized nominal strength $\sigma_N = P/h^2$ versus the relative thickness of the ice (note that according to plasticity or elasticity with strength criterion, this plot would be a horizontal line). The initial horizontal portion, for which there is no size effect, corresponds to ice thinner than about 20 cm.

Since the model of Bažant and Kim includes plasticity, it can reproduce the classical solutions with no size effect, depending on the input values of ice characteristics. The ice thickness at the onset of size effect depends on the ratio of ice thickness to the fracture characteristic length, h/l_0. For realistic ice thicknesses h ranging from 0.1 m to 6 m, the computer program would yield perfectly plastic response with no size effect size effect if the fracture characteristic length l_0 were at least 100× larger, i.e., at least 25 m. This would, for instance, happen if either f'_t were at least 10× smaller ($f'_t \leq 0.01$ MPa or K_c at least 10× larger ($K_c \geq 10$ MPa $\sqrt{\text{m}}$). The entire diagram in Fig. 1g would then be horizontal.

Larger values of l_0 are of course possible in view of statistical scatter, but nothing like 100× larger. For example, by fitting Dempsey et al.'s (2000b) size effect data from in-situ tests at Resolute, one gets $K_c \approx 2.1$ MPa $\sqrt{\text{m}}$, and with $f'_t \approx 2$ MPa one has the fracture characteristic length $l_0 = (K_c/f'_t)^2 = 1$ m. But this larger value would not make much difference in the size effect plot in Fig. 1g. The reason that these values were not used in the plot in Fig. 1g was that they correspond to long-distance horizontal propagation of fracture, rather than vertical growth of fracture.

The curve in Fig. 1g is the optimum fit of the numerically calculated data points by the generalized size effect law proposed in Bažant (1985). The final asymptote has slope $-1/2$, which means that the asymptotic size effect is $\sigma_N \propto h^{-1/2}$, the same as for LEFM with similar cracks, and not $h^{-3/8}$ as proposed by Slepyan (1990), Bažant (1992) and Bažant and Li (1994). The $-3/8$ power scaling would have to be true if the radial cracks at maximum load were full-through bending cracks. The $-1/2$ power scaling may be explained by the fact that during failure the bending cracks are not full-through and propagate mainly vertically, which is supported by the calculated crack profiles in Fig. 1e.

By fitting of the data points in Fig. 1g, spanning over four orders of magnitude of ice thickness h, the following prediction formula in the form of the generalized size effect law (Bažant 1985; Bažant and Planas 1998) has been calibrated (see the curve in Fig. 1g):

$$P_{max} = \sigma_N h^2, \quad \sigma_N = B f'_t \left[1 + (h/\lambda_0 l_0)^r\right]^{-1/2r} \tag{3}$$

with $B = 1.214$, $\lambda_0 = 2.55$, $m = 1/2$, $r = 1.55$ and $l_0 = 0.25$ m ($f'_t = 0.2$ MPa in Fig. 2).

Only very limited field test data exist. The data points in the size effect plots in Fig. 1h represent the results of the field tests by (Frankenstein 1963,1966) and Lichtenberger (1974), and the curves show the optimum fits with the size effect formula verified by numerical calculations (note that if the size effect were absent, these plots of nominal strength would have to be horizontal). After optimizing the size effect law parameters by fitting the data in the three plots in Fig. 1h, the data and the optimum fit are combined in the dimensionless plot in Fig. 1i.

Interesting discussions of Bažant and Kim's (1998) study were published by Dempsey (2000) and Sodhi (2000) and rebutted by the authors. One objection

raised by Sodhi was the neglect of creep in Bažant and Kim's analysis. Intuition suggests that the influence of creep might be like that of plasticity, which tends to increase the process zone size, thereby making the response less brittle and the size effect weaker. But the influences of creep and plasticity are very different.

The influence of creep on scaling of brittle failures of concrete, which is doubtless quite similar from the mechanics viewpoint (albeit different in physical origin), was studied in depth at Northwestern University, along with the effect of the crack propagation velocity; see e.g. Bažant and Gettu (1992); Bažant et al. (1993); Bažant and Planas 1998; and especially Bažant and Li (1997), and Li and Bažant (1997). The conclusion from these studies, backed by extensive fracture testing of concrete and rock at very different rates, is that (unless creep actually prevents crack initiation) creep in the material always makes the size effect due to cracks stronger. In the logarithmic size effect plot of nominal strength versus structure size, it causes a shift to the right, toward the LEFM asymptote, which means that the size effect is intensified by creep. The slower the loading (or the longer its duration), the closer to LEFM is the size effect in a cracked structure.

The physical reason, clarified by numerical solutions of stress profiles with a rate-dependent cohesive crack model (Li and Bažant 1997), is that the highest stresses in the fracture process zone get relaxed by creep, which tends to reduce the effective length of the fracture process zone. The shorter the process zone, the higher is the brittleness of response and the stronger is the size effect. This explains why experiments on notched concrete specimens consistently show the size effect to be more pronounced at a slower loading (Bažant and Planas 1998). A similar behavior might be expected for ice. It thus transpires that, in order to take the influence of creep on the size effect approximately into account, it suffices to reduce the value of fracture energy (or fracture toughness) and decrease the effective length of the fracture process zone.

2.2 Approximate Analytical Solution of the Vertical Penetration Problem

An ice plate floating on water behaves exactly as a plate on Winkler elastic foundation (Fig. 2a,b), with a foundation modulus equal to the specific weight of water, ρ. Failure under a vertical load is known to involve formation of radial bending cracks in a star pattern (shown in a plan view in Fig. 2c for the case of 6 cracks). As transpired from a simplified analytical study of Dempsey et al. (1995) and was shown in a detailed numerical simulation by Bažant and Kim (1998), these radial cracks do not reach through the full ice thickness before the maximum load is reached. Rather, they penetrate at maximum load to an average depth of about $0.8h$ and maximum depth $0.85h$ where h is the ice thickness (Fig. 3a). The maximum load is reached when polygonal (circumferential) cracks, needed to complete a failure mechanism, begin to form (dashed lines in Fig. 2c).

Sea ice, unlike glacier ice, is not sufficiently confined to behave plastically. It is a brittle material, and so the failure must be analyzed by fracture mechanics (e.g. Dempsey 1991; DeFranco and Dempsey 1992, 1994; DeFranco et al. 1991; Bažant 1992a,b; Bažant and Li, 1994; Li and Bažant 1994; Bažant and Kim 1998). The analysis must be based on the rate of energy dissipation at the crack front and the rate of energy release from the ice-water system. The energy release is associated with unloading, during which the ice deforms elastically, with a certain Young's modulus E (which depends on temperature and other factors).

The behavior of the ice plate may be described by the plate bending theory. Dimensional analysis, or transformation of the partial differential equation of a

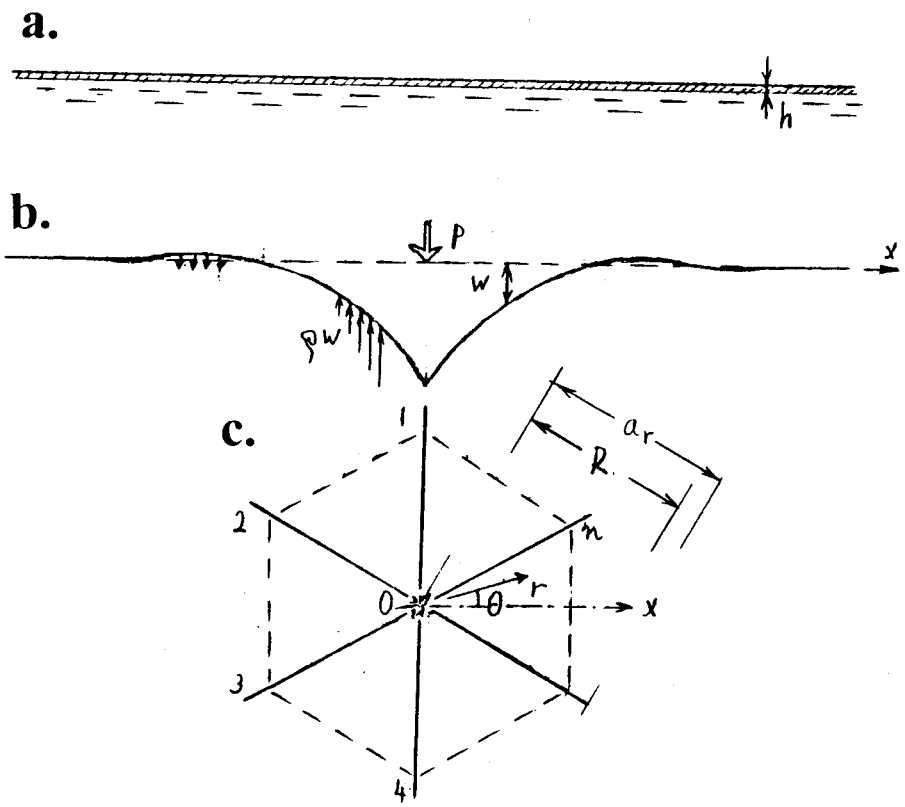

Figure 2: Floating ice plate, its deflection under concentrated load and crack pattern.

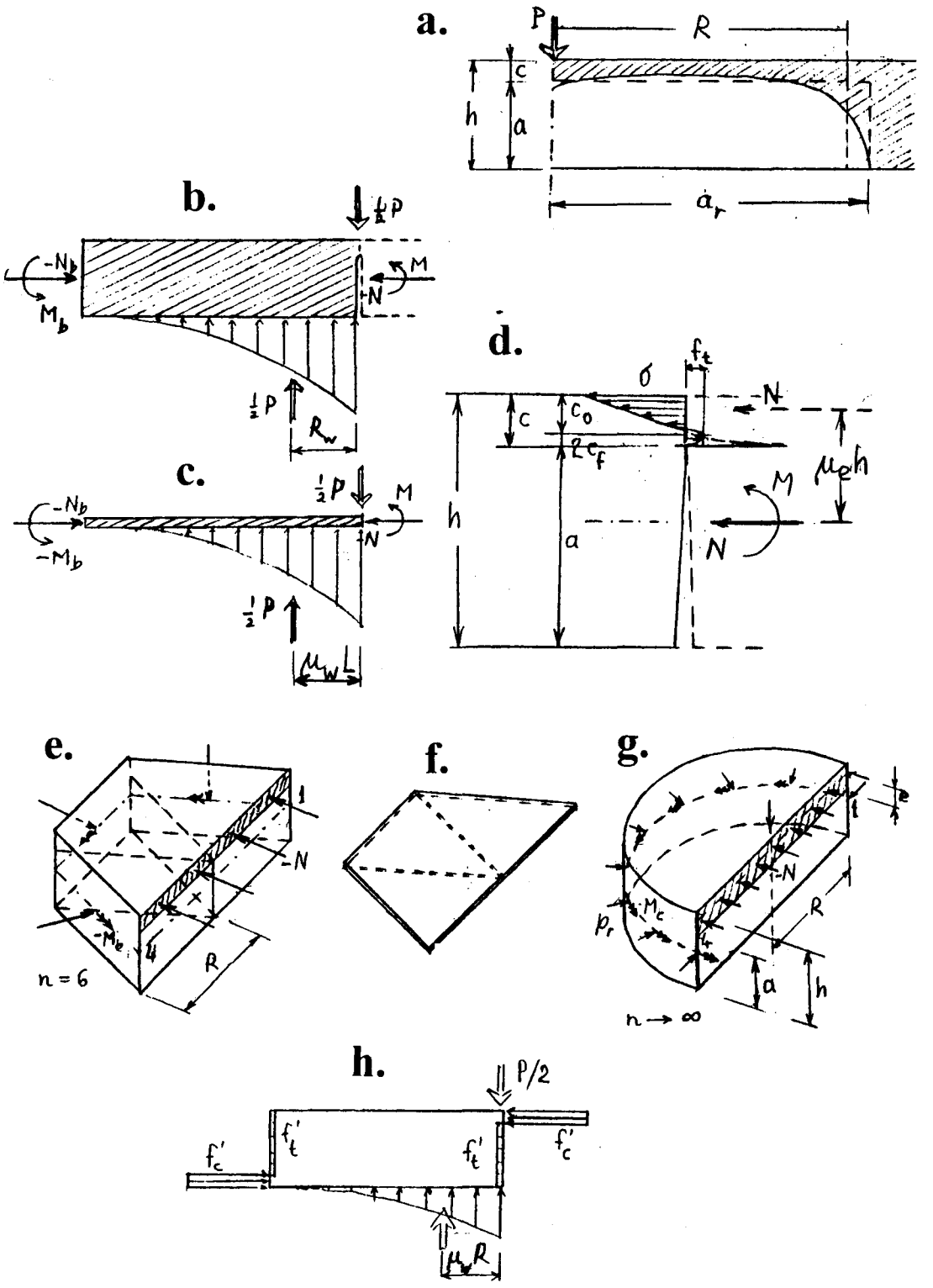

Figure 3: Analysis of vertical penetration fracture: (a) Crack profile and (b-h) forces acting on element 123401.

plate on Winkler foundation to dimensionless coordinates, shows that the behavior of the plate is fully characterized by the characteristic length

$$L = (D/\rho)^{1/4} \tag{4}$$

where $D = Eh^3/12(1-\nu^2)$ = cylindrical stiffness of the ice plate; ν = Poisson ratio of ice.

Superposing the expressions for the stress intensity factor K_I of the part-through radial bending crack of depth a (Fig. 1b) produced by bending moment M and normal force N (per unit length), one has

$$K_I = \frac{\sqrt{\pi a}}{h}\left[\frac{6M}{h}F_M(\alpha) + NF_N(\alpha)\right] \tag{5}$$

where (Tada et al. 1985)

$$F_M(\alpha) = \sqrt{\frac{2}{\pi\alpha}\tan\frac{\pi\alpha}{2}}\left(\cos\frac{\pi\alpha}{2}\right)^{-1}\left[0.923 + 0.199\left(1-\sin\frac{\pi\alpha}{2}\right)^4\right] \tag{6}$$

$$F_N(\alpha) = \sqrt{\frac{2}{\pi\alpha}\tan\frac{\pi\alpha}{2}}\left(\cos\frac{\pi\alpha}{2}\right)^{-1}\left[0.752 + 2.02\alpha + 0.37\left(1-\sin\frac{\pi\alpha}{2}\right)^3\right] \tag{7}$$

with an error less than 0.5% over the entire range $\alpha \in (0,1)$. According to Irwin's relation, the energy release rate is

$$\mathcal{G} = \frac{K_I^2}{E'} = \frac{N^2}{E'h}g(\alpha) \tag{8}$$

where $E' = E/(1-\nu^2)$ and g is a dimensionless function,

$$g(\alpha) = \pi\alpha\left[\frac{6e}{h}F_M(\alpha) + F_N(\alpha)\right]^2 \qquad (\alpha = a/h) \tag{9}$$

$e = -M/N$ = eccentricity of the normal force resultant in the cross section (positive when N is above the mid-plane).

To relate M and N to vertical load P, let us consider element 12341 of the plate (Fig. 2c and 3e,f,g), limited by a pair of opposite radial cracks and the initiating polygonal cracks. The depth to the polygonal cracks at maximum load is zero, as they just initiate, and since the cracks must form at the location of the maximum radial bending moment, the vertical shear force on the planes of these cracks is zero. The distance R of the polygonal cracks from the vertical load P must be proportional to the characteristic length L since this is the only constant in the differential equation governing the problem, and so we may set $R = \mu_R L$ where dimensionless μ_R is assumed to be a constant.

In each narrow radial sector, the resultant of the water pressure due to deflection w (Fig. 3b,c) is located at a certain distance r_w from load P. Since r_w can be solved from the differential equation for w, and since the solution depends only on one parameter, the characteristic length L, r_w must be proportional to L. Integration over the area of a semi-circle of radius r_w yields the resultant of water pressure acting on the whole element 12341. Again, the distance of this resultant, whose magnitude it $P/2$, from load P must be proportional to L, i.e., may be written as

$$R_w = \mu_w L \tag{10}$$

where μ_w is a constant that can be solved from the differential equation of plate deflections. Of course, μ_w is a constant only as long as the behavior is elastic. This is exactly true only if the crack depth a is constant. Although the crack is growing, we will assume that its rate of growth is small enough so that μ_w would be approximately constant.

For the sake of simplicity, we assume the normal force N and bending moment M on the planes of the radial cracks and the polygonal cracks to be uniform. The condition of equilibrium of horizontal forces acting on element 12341 in the direction normal to the radial cracks is then simple; it requires the normal forces on the planes of the polygonal cracks to be equal to the normal force N acting in the radial crack planes. The axial vectors of the moments M_c acting on the polygonal sides are shown in Fig. 3e,g by double arrows. Summing the projections of these axial vectors from all the polygonal sides of the element, one finds that their moment resultant with axis in the direction 14 is $2RM_c$, regardless of the number n of radial cracks. So, upon setting $R = \mu_R L$, the condition of equilibrium of the radial cracks with the moments about axis 14 (Fig. 3b,c,e,g) located at mid-thickness of the cross section may be written as:

$$2(\mu_R L)M + 2(\mu_R L)M_c - \tfrac{1}{2}P(\mu_w L) = 0 \tag{11}$$

The polygonal cracks initiate when the normal stress σ reaches the tensile strength f_t' of the ice. As in all heterogeneous brittle materials, one must expect that a layer of distributed microcracking, of some effective constant thickness D_b that is a material property, will form at the top face of ice plate before the polygonal crack will start propagating (the existence of such a layer has been shown to explain the size effect on the modulus of rupture in the bending tests of concrete; Bažant and Li 1996). According to the nonlocal concept for distributed damage, we may thus more generally assume that the polygonal cracks initiate when the average stress in this layer reaches the strength f_t', and since the average stress is roughly the elastically calculated stress for the middle of layer D_b, the criterion of initiation of the polygonal cracks may be written according to the theory of bending simply as

$$\frac{M_c}{h^3/12}\left(\frac{h}{2} - \frac{D_b}{2}\right) + \frac{N}{h} = f_t' \tag{12}$$

This criterion, however, cannot be valid when $h < D_b$, i.e., the cracking zone tends to be larger than the cross section. It can be correct only when h is sufficiently larger than D_b, i.e., asymptotically for $h/D_b \to \infty$. The case $h < D_b$ is physically meaningless. For $h = D_b$, i.e., when the distributed cracking zone encompasses essentially the whole depth of plate, the moment at failure can be determined as the plastic bending moment, which may be approximately taken as 1.5× larger than the elastic bending moment for the same material strength. This condition and the asymptotic properties for $h \gg D_b$ are satisfied by replacing (12) with the criterion:

$$\frac{6M_c}{h^2}\frac{h + D_b}{h + 2D_b} + \frac{N}{h} = f_t' \tag{13}$$

Indeed, by expanding the left-hand side as Taylor series in $\xi = h/D_b$ and keeping only its first two terms, one obtains (12). This means that these two expressions are equivalent asymptotically, for large enough ξ.

In (11), we may substitute

$$M = -Ne = N\mu_e h \tag{14}$$

where $\mu_e = e/h$ = dimensionless parameter whose value at maximum load may be assumed as approximately constant. This assumption is indicated by the numerical simulation of Bažant and Kim (1998), from which it further transpires that $\mu_e \approx 0.45$, as a consequence of the fact the average crack depth a at maximum load is about $0.8h$. N is defined, as customary, to be positive when tensile, although the actual value of N is negative (compression). After substituting (14), we may express M_c from (11) and substitute it into (13).

Furthermore, we must take into account the condition (8) of vertical propagation of the radial bending cracks, which may be written as $\mathcal{G} = G_f$ where G_f is the fracture energy of ice. Thus, the critical value of normal force (compressive, with eccentricity e) may be written as

$$N = -\sqrt{\frac{E'G_f h}{g(\alpha)}} \tag{15}$$

The aforementioned operations furnish the equation

$$\frac{3(h+D_b)\mu_w}{2h(h+2D_b)\mu_R}\sigma_N = \left(\frac{6\mu_e(h+D_b)}{h^2(h+2D_b)} + \frac{1}{h}\right)\sqrt{\frac{E'G_f h}{g(\alpha)}} + f'_t \tag{16}$$

which may be rearranged as

$$\sigma_N = \frac{2\mu_R}{3\mu_w}\left\{\left[6\mu_e + \frac{h+2D_b}{h+D_b}\right]\sqrt{\frac{E'G_f}{hg(\alpha)}} + f'_t\frac{h+2D_b}{h+D_b}\right\} \tag{17}$$

Finally, one needs to decide how the values of α at maximum load should change with ice thickness h. To this end, note that ice is a quasibrittle material. This is evidenced by the fact that at small laboratory scale it is notch-insensitive and exhibits no size effect while at large scale it behaves according to linear elastic fracture mechanics (LEFM) (Dempsey 1989, Dempsey et al. 1999b). Therefore, at the tip of the vertically propagating radial crack, there must exist a finite fracture process zone (FPZ) of a certain characteristic depth $2c_f$ which is a material property. This zone was modeled in the numerical simulations of Bažant and Kim (1998) as a yielding zone. The tip of the equivalent LEFM crack lies approximately in the middle of the FPZ, i.e., at a distance c_f from the actual crack tip (Bažant and Planas 1998), whose location is denoted as a_0. In structures of different sizes, the locations of the center of FPZ are usually not geometrically similar; rather, similar locations are those of the actual crack tip, i.e., the value of $\alpha_0 = a_0/h$ may be expected to be approximately constant when ice plates of different thicknesses h are compared. Thus, denoting $g'(\alpha_0) = \mathrm{d}g(\alpha_0)/\mathrm{d}\alpha_0$, one may introduce the approximation

$$g(\alpha) \approx g(\alpha_0) + g'(\alpha_0)c_f \tag{18}$$

Substituting this into (17) and rearranging, one gets

$$\sigma_N = \frac{4\mu_R}{\mu_w}\left[\mu_e + \frac{h+2D_b}{6(h+D_b)}\right]\sqrt{\frac{E'G_f}{hg(\alpha_0)+c_f g'(\alpha_0)}} + \frac{\mu_R}{3\mu_w}\frac{h+2D_b}{h+D_b}f'_t \tag{19}$$

The results of numerical simulations of Bažant and Kim (1998) were found to be quite well represented by the simple classical size effect law proposed for

quasibrittle fracture by Bažant (1984), which reads:

$$\sigma_N = \sigma_0 \left(1 + \frac{h}{h_0}\right)^{-1/2} + \sigma_r \tag{20}$$

where σ_r is the large-size residual strength, which appeared to be negliglible in Bažant and Kim's (1998) numerical simulations (although in some problems of concrete it is not). Equation (19) reduces to this law with $\sigma_r = 0$ when $D_b = 0$ and $f_t' = 0$, in which case then

$$\sigma_0 = \frac{4\mu_R\mu_e}{\mu_w}\sqrt{\frac{E'G_f}{c_f g'(\alpha_0)}}, \qquad h_0 = c_f \frac{g'(\alpha_0)}{g(\alpha_0)}, \qquad \sigma_r = \frac{\mu_e}{3\mu_w} f_t' \tag{21}$$

This means that the values of D_b and f_t' are probably too small to have an appreciable effect.

The terms in (19) containing D_b anyway decrease with increasing h much more rapidly than (20)—for large h as $1/h$ compared to $1/\sqrt{h}$. Consequently, they must become negligible for sufficiently large h regardless of the value of D_b. Same as (20), equation (19) plotted as $\log \sigma_N$ versus $\log h$ approaches for large h a downward inclined asymptote of slope $-1/2$ and represents the large-size form of the size effect law in (19).

Compared to the previous numerical simulations, the present derivation is instructive in clarifying the reasons why there must be a deterministic size effect in penetration of floating ice. The size effect could be absent only if the failure occurred at the initiation of fracture, not after a large stable crack growth, of if the material behaved plastically. The stress distributions on element 12341 for the case of plastic failure are shown in Fig. 3h, where f_t', f_c' denote the tensile and compressive yield strengths. Taking the moment equilibrium condition of this element, one can show that the nominal strength would in that case be expressed as

$$\sigma_N = \frac{4\mu_R}{\mu_w}(f_c'^{-1} + f_t'^{-1})^{-1} \tag{22}$$

which exhibits no size effect. In a brittle material such as ice, however, the strength cannot be mobilized at various points at the same time, and so this solution cannot apply to ice.

How does the number n of the radial cracks enter the solution? It does not appear in the present solutions for the maximum load. The reason is that the number of cracks is decided at the beginning of loading, long before the maximum load is attained.

It is interesting to contrast the size effect obtained here with that deduced for large-scale thermal bending fracture of floating ice, which was shown to be (Bažant 1992)

$$\Delta T \propto h^{-3/8} \tag{23}$$

where ΔT is the temperature difference between the bottom and top of the ice plate, which is proportional to the maximum thermal stress before fracture. The large-size asymptotic size effect for fracture under vertical loads would have to follow also the $-3/8$ power law if the cracks at maximum load penetrated through the full thickness of ice and N were negligible (Slepyan 1990, Bažant 1992, Bažant and Li 1994), but this turned out not to be the case (Dempsey at el. 1995, Bažant and Kim 1998).

3 Force Applied by Moving Ice Plate on a Fixed Structure

Another fundamental problem where the question of scale is or prime interest is the force P that a moving and breaking ice plate of thickness h exerts on a fixed structure, idealized as a circular cylinder of diameter d. The nominal strength of the structures may in this case be defined as the average stress on the cross section area hd of the structure facing the ice plate, i.e.,

$$\sigma_N = P/hd \tag{24}$$

Several mechanisms of break-up are possible.

3.1 Global Failure Due to Buckling of Ice Plate

Cylindrical buckling, in which the deflection surface is a translationary surface, can occur only if the ice plate is moving against a long wall ($d \to \infty$) . In this case the plate behaves as a beam on elastic foundation, which is a one-dimensional problem, and the critical compressive normal force per unit width of the plate is known to be (e.g. Bažant and Cedolin 1991) $N_{cr} = \kappa_0\sqrt{\rho D}$ where coefficient κ depends on the boundary conditions. Its smallest possible value, which corresponds to a sinusoidal buckling mode, is $\kappa_0 = 2$.

If the obstacle, such as the legs of an oil drilling platform, has a finite dimension d in the transverse direction, the buckling mode is two-dimensional and more complicated. In any case, however, dimensional analysis (Sedov 1959, Barenblatt 1987) suffices to determine the form of the buckling formula and the scaling. There are five variables in the problem, P_{cr}, E', ρ, h, d, and the solution must be have the form $F(P_{cr}, E', \rho, h, d) = 0$, where $E' = E/(1-\nu^2)$ and P_{cr} is the critical force exerted by the resisting structure on the moving ice plate (Fig. 4a).

There are, however, only two independent physical dimensions in the problem, namely the length and the force. Therefore, according to Buckingham's Π theorem of dimensional analysis (Barrenblatt 1979, 1987; Sedov 1959), the solution must be expressible in terms of $5-2$, i.e., 3 dimensionless parameters. They may be taken as $P_{cr}/E'hd$, $\sqrt{\rho D}/E'h$ and d/h. Because the buckling is linearly elastic, $P_{cr}/E'hd$ must be proportional to $\sqrt{\rho E'}/E'h$ and d/h. Denoting

$$\sigma_{N\,cr} = P_{cr}/hd \tag{25}$$

which represents the nominal buckling strength (or the average critical stress applied by face of the resisting structures on the moving ice plate), and noting that $D = E'h^3/12$ with $E' = E/(1-\nu^2)$, we conclude that the buckling solution must have the form

$$\sigma_{N\,cr} \;=\; \kappa(d/h)\,\sqrt{\rho E'}\,\sqrt{h} \tag{26}$$

where κ is a dimensionless parameter depending on the relative diameter of the structure, d/h, as well as on the boundary conditions. For $h/d \to \infty$ (an infinite wall), this must reduce to the solution for a beam on elastic foundation, and so $\kappa(0)/\sqrt{12} = 2$ or $\kappa(0) = 4\sqrt{3}$. This represents the smallest possible value of κ for any d/h, which becomes obvious by imagining a strip of width d in the direction of movement to be separated from the rest of the ice plate; for that strip $\kappa_0 = 2$, and re-attaching the rest of the plate must increase the critical load.

The interesting property of (26) is that $\sigma_{N\,cr}$ increases, rather than decreases, with ice thickness h. So there is a reverse size effect. Consequently, the buckling of the ice plate can control the force exerted on a stationary structure only when the

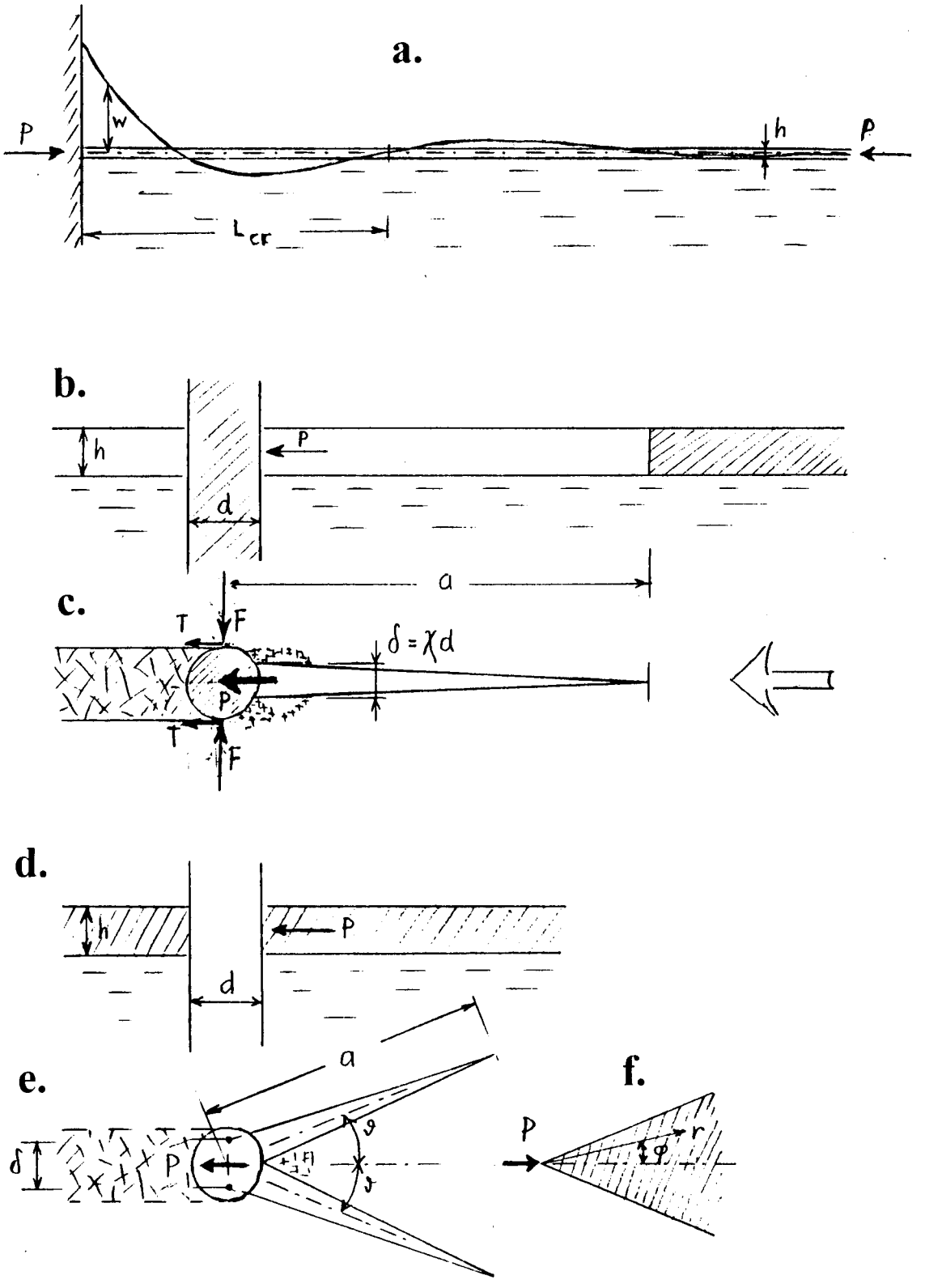

Figure 4: (a) Buckling of ice plate pushing horizontally against a fixed structure, and (b,c) cleavage crack, and (d-f) diverging V-cracks.

plate is sufficiently thin. The reason for the reverse size effect is that the buckling wavelength (the distance between the inflexion points of the deflection profile), which is $L_{cr} = \pi(D/\rho)^{1/4}$ (as follows from dimensional analysis or nondimensionalization of the differential equation of plate buckling), is not proportional to h; rather

$$L_{cr}/h \propto h^{-1/4} \tag{27}$$

i.e., L_{cr} decreases with h. This contrasts with the structural buckling problems of columns, frames and plates, in which L_{cr} is proportional to the structure size.

3.2 Global Failure Due to Cleavage Fracture

Another failure mechanism consists of a long cleavage crack in the ice plate, propagating against the direction of ice movement (Fig. 4b,c). The resistance of the cracks to opening causes the ice to exert on the structure a pair of transverse force resultants F and a pair of tangential forces T in the direction of movement; $T = F\tan\varphi$ where φ nay be regarded as the friction angle. Forces T have no effect on the stress intensity factor K_I at the crack tip. Considering the ice plate as infinite, we have

$$K_I = \frac{F}{h}\sqrt{\frac{2\pi}{a}} \tag{28}$$

(Tada et al. 1985, Murakami 1987). To determine the crack length a (Fig. 4b,c), we need to calculate the crack opening δ caused by F. To this end, one may recall the well-known calculation of the energy release rate:

$$\mathcal{G} = \frac{1}{h}\left[\frac{\partial \Pi *}{\partial a}\right]_F = \frac{1}{h}\frac{\mathrm{d}}{\mathrm{d}a}\left[\tfrac{1}{2}C(a)F^2\right] = \frac{F^2}{2h}\frac{\mathrm{d}C(a)}{\mathrm{d}a} \tag{29}$$

where $C(a)$ is the load-point compliance of forces F. Upon using (28) and Irwin's relation, we have at the same time

$$\mathcal{G} = \frac{K_I^2}{E} = \frac{2\pi F^2}{Eh^2 a} \tag{30}$$

Equating (29) and (30), we thus get

$$\frac{\mathrm{d}C(a)}{\mathrm{d}a} = \frac{4\pi}{Eha} \tag{31}$$

This expression is now integrated from $a = d/2$ (surface of structure, considered as circular (Fig. 4b,c) to a (note that integration from $a = 0$, which would give infinite C, would be meaningless because a cannot be less than d). In this manner we obtain $C(a)$, and from it the opening deflection δ:

$$\delta = C(a)F = \frac{4\pi F}{Eh}\ln\left(\frac{2a}{d}\right) \tag{32}$$

If cleavage fracture were the only mode of ice breaking, we would have $\delta = d$. However, as will be discussed later, there is likely to be at least some amount of

local crushing at, and ahead, of the structure. Consequently, the relative displacement between the two flanks of the crack is no doubt less that d. We denote it as χd where χ is a coefficient less than 1. Setting $\delta = \chi d$, we solve from (32):

$$a = \frac{d}{2} \exp\left(\frac{Eh\chi d}{4\pi F}\right) \tag{33}$$

(note that a/d is not constant but increases with d; hence, the fracture modes are not geometrically similar, and so the LEFM power scaling cannot be expected to apply). Substituting (33) into (28), setting $K_I = K_c = \sqrt{EG_f}$ (Irwin's relation, K_c = fracture toughness of ice), and solving for F, we obtain

$$\frac{2\sqrt{\pi}F}{h\sqrt{EG_f d}} = \exp\left(\frac{Eh\chi d}{8\pi F}\right) \tag{34}$$

The pair of forces F is related to load P on the structure ($P = 2T$, Fig. 4c) by a friction law, which may be written as

$$P = 2\,F\,\tan\varphi \tag{35}$$

where φ is the friction angle. Substituting $F = P/2\tan\varphi$ and $P = \sigma_N hd$ into (34), and solving the resulting equation for d, we obtain, after rearrangements,

$$\frac{d}{d_c} = \frac{1}{\tau^2}\, e^{1/\tau}, \qquad \tau = \frac{\sigma_N}{\sigma_c} \tag{36}$$

in which τ is the dimensionless nominal strength, and d_c and σ_c are constants defined as

$$d_c = \frac{4\pi G_f}{\chi^2 E}, \qquad \sigma_c = \frac{\chi \tan\varphi}{2\pi}\, E \tag{37}$$

Equation (36), plotted in Fig. 5, represents the law of cleavage size effect in an inverted form. The small-size asymptotic behavior is the LEFM scaling for similar structures with similar cracks:

$$\text{for } d \ll d_c\text{:} \quad \sigma_N \approx \sqrt{d_c/d}; \tag{38}$$

The plot of (36) in Fig. 5 shows that the size effect is getting progressively weaker with increasing structure diameter d (although no horizontal asymptote is approached by the curve). The reason for this is that the crack is dissimilar, i.e., the ratio, a/d, of crack length to structure diameter is not the same for different sizes but increases according to (33) with the structure size. In designing ocean platforms, it is nevertheless always advantageous, with respect to the cleavage mechanism, to use a smaller number of larger legs (which has of course been intuitively followed in practice).

3.3 Compression Fracture of Ice Plate

As typically observed in the field, ice breaks up into chunks in front of an obstacle. The cause is local compression fracture of the material. Its initiation is explained by sliding on inclined weak plains between ice crystals, which leads to axial splitting microcracks called the wing-tip cracks (for ice, see e.g. Schulson 1990, 2000)

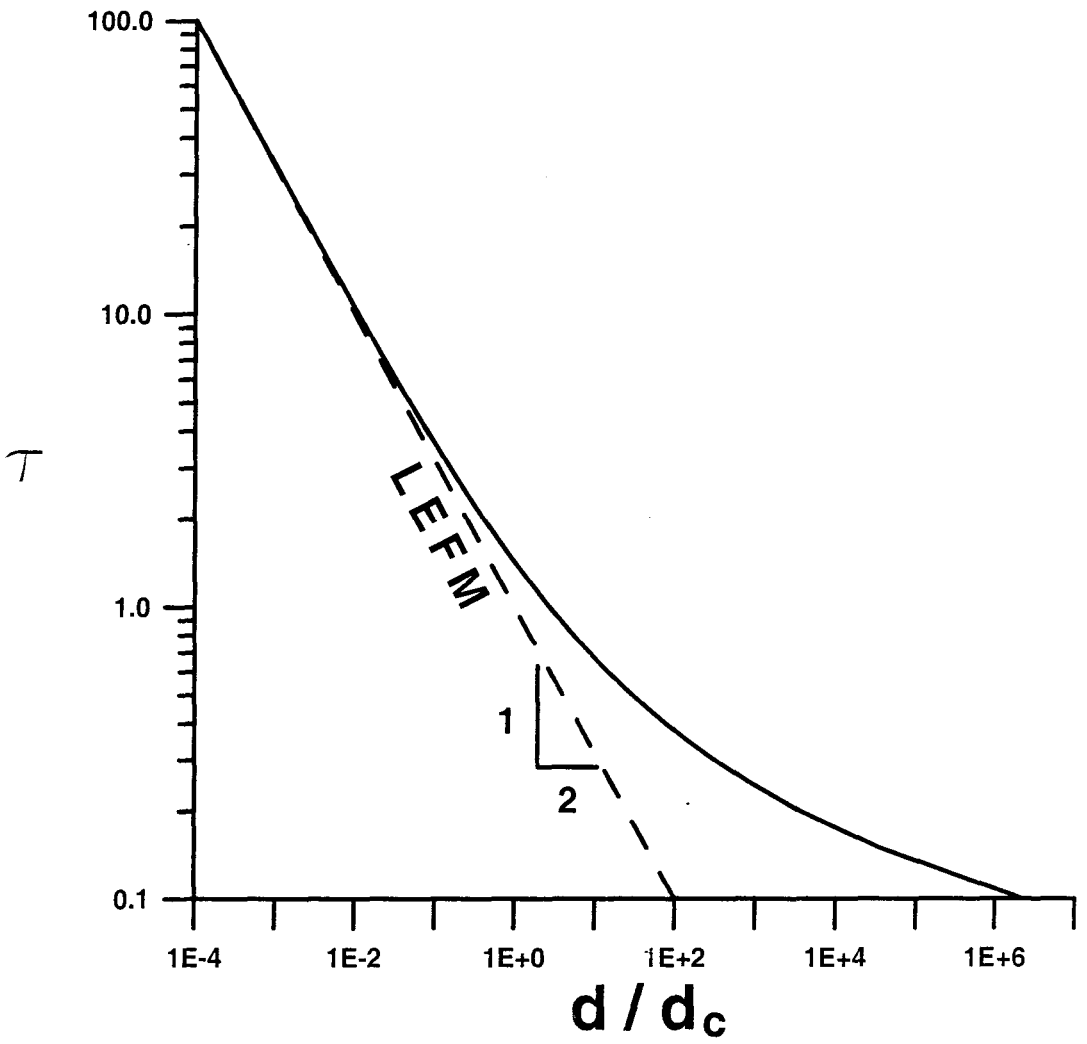

Figure 5: Size effect associated with cleavage fracture.

extending in the direction of compression for a certain finite length. This mechanism, however, explains only the generation of local compressive damage in the material but does not explain to overall failure of the plate.

To produce overall failure, the damage must propagate. The propagation typically occurs in the form of a narrow band consisting predominantly of axial splitting microcracks (generated by the wing-tip crack mechanism). The band of axial splitting microcracks can propagate either in the axial direction of the compressive stress, or laterally. The latter is shown in Fig. 6a, and the former in Fig. 6b.

In the spirit of fracture mechanics, one must estimate the energy release. Consider the plausible situation depicted in Fig. 6a, where the band of a certain characteristic width w_c in the direction of compression has inclination ψ_b and reaches to depth a below the surface of plate. Formation of the band relieves the axial stress σ_N not only within the band area 12541, but also in the adjacent zones 1231 and 4564. The boundary of the stress relief zone is considered to have a certain characteristic inclination ψ_a, independent of the plate thickness. The combined area of the stress relief zone 43264 is $a(w_c + \frac{1}{2}a\tan\psi_a + a\tan\psi_b)$. Before the formation of the damage band, the initial strain energy density in this zone is $\sigma_N^2/2E$, and after the formation of the band it may be assumed as zero (more generally, one could assume some residual stress σ_r after crushing, which however would lead to similar results; see Bažant and Xiang 1997). Thus the total energy release caused by formation of the damage band per unit width is, approximately,

$$\Pi^* = \frac{\sigma_N^2}{2E}\, a\ \left(w_c + \tfrac{1}{2}a\tan\psi_a + a\tan\psi_b\right) \tag{39}$$

The rate of energy dissipation per unit width as the band propagates must be equal to the fracture energy of the band, G_b, which equals $G_f w_c/s_c$ where G_b is the fracture energy of the axial splitting microcracks in the band, and s_c their average spacing. Energy balance during the quasistatic extension of the band requires that the rate of energy release be equal to G_f, i.e.,

$$\frac{\partial\Pi^*}{\partial a} = \frac{\sigma_N^2}{2E}(w_c + a\tan\psi_a + 2a\tan\psi_b) = G_b \tag{40}$$

Solving this equation for σ_N, we get, after rearrangements,

$$\sigma_N = \sigma_a\left(1 + \frac{h}{h_0}\right)^{-1/2} \tag{41}$$

in which the following notations are made

$$h_0 = \frac{h}{a}\,\frac{w_c}{(\tan\psi_a + 2\tan\psi_b)}, \qquad \sigma_a = \sqrt{\frac{2EG_c}{w_c}} \tag{42}$$

Here we deliberately introduced the plate thickness h even though it cancels out of the equation. The reason is that it appears reasonable to assume the ratio a/h for plates of various thicknesses to be approximately constant. In other words, the geometries of the damage band at failure of the plates of various thicknesses are assumed similar. This assumption is based on experience with some fracture problems, for which it was shown to lead to realistic results. Anyway, it is intuitively clear that it would be unreasonable to assume that for thin plates the damage band at maximum σ_N penetrates through most of the thickness and for thick plates penetrates only to a very shallow depth.

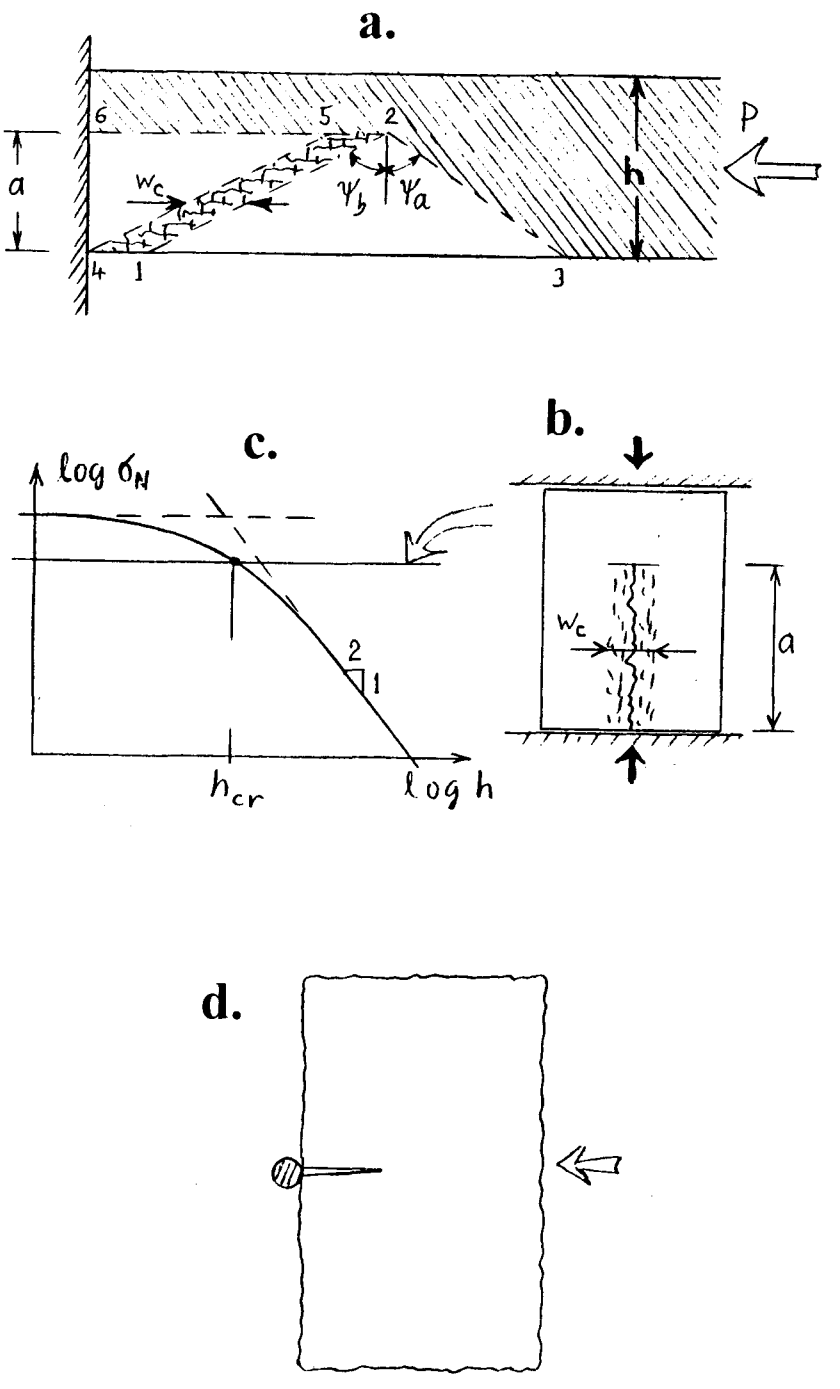

Figure 6: (a) Compression fracture of ice plate, (b) axial splitting fracture, (c) size effects corresponding to (a) and (b), and (d) overall fracture of ice floe.

Equation (41), plotted in Fig. 6c, is the same as the classical size effect law proposed by Bažant (1984) for quasibrittle structures failing after a long stable growth of tensile fracture. Among the mechanisms explored here, it is the only one that can explain the size effect of ice thickness.

The ultimate cause of size effect in compressive (as well as tensile) fracture is that the volume of the energy dissipation zone, i.e. the damage band, grows linearly with the distance a of propagation while the volume of the energy release zone grows faster than linearly, having a quadratically growing term that dominates for large sizes. Thus it is intuitively clear that if the stress in these zone at failure were the same, energy balance could exist only for one size but not for other sizes (Bažant and Chen 1997). So, in a larger structure the stress in the quadratically growing zones (1231 and 4564 in Fig. F5a) must be less.

There is of course another possibility—namely that the damage band grows axially, in the direction of compression, which leads to a splitting failure (Fig. 6b). In that case the stress in the material on the sides of the crack band is not relieved, and so the energy release occurs only within the damage band itself. Not only the energy dissipation but also the energy release are proportional to the length a of the band, which means that energy rates for the same failure stress σ_N can balance for any size h. In that case there is no size effect.

The axial growth is more likely because no new wing-tip cracks need to be nucleated. Therefore, at small enough sizes the axial splitting of ice should prevail, which means that the splitting mechanism corresponds in the logarithmic size effect plot (Fig. 6c) to a horizontal line starting below the curve of the size effect law for lateral propagation of the damage band. However, the horizontal line must eventually cross the curve at a certain critical size h_{cr}, above which the lateral propagation of damage band must prevail, and then a size effect must exist.

The present analysis is similar to that made for concrete; seeBažant and Xiang 1997, where various fine details are discussed (also Bažant and Planas 1998, Bažant and Chen 1997).

Finally, an explanation of empirical parameter χ introduced for the cleavage fracture: It is presumed that the part $(1-\chi)d$ of the cross section facing the ice movement undergoes compression crushing. This part should be governed by equation (41), and so the force given by that equation needs to be added to the force P based on (35) and (36).

3.4 Overall Fracture of Finite Ice Floe

Collision of a large ice floe with a fixed structure may cause a fracture of the whole floe. The floe is loaded by distributed inertia forces of its mass, but the problem may be treated as essentially quasistatic, owing to the low velocity of movement. Except for the loading by distributed forces, the problem is similar to fracture tests in the laboratory, especially the three-point bend beam (Fig. 6d). Dempsey's record-breaking tests on the Arctic Ocean near Resolute can be regarded as an approximate reduced-scale simulation of this kind of fracture (Dempsey et al. 1999b, Mulmule et al. 1995). The analysis may follow similar lines as presented, for instance, by Bažant and Planas (1998) for other materials. From that analogy it follows that the size L of the floe may cause one of two types of size effect:

$$1) \qquad \frac{P}{Lh} = S_0\left(1+\frac{L^r}{L_0^r}\right)^{-1/2r} \tag{43}$$

$$2) \qquad \frac{P}{Lh} = S_\infty \left(1 + \frac{rL_b}{L}\right)^{1/r} \tag{44}$$

where P/Lh is the nominal strength of the whole floe; S_0, L_0, S_∞, L_b are constants that can be calculated by fracture mechanics; and r is a parameter whose value is normally between 0.5 and 2.

The first kind of size effect, which agrees very well with Dempsey et al.'s (1999b) field tests in the Arctic, applies when a large crack in the floe can form before the overall fracture of the floe takes place. The second kind applies to failures at fracture initiation, exemplified by the test of modulus of rupture (bending strength), and is pertinent if the floe fractures the maximum load is attained before a stable finite crack can develop (e.g, by means of the cleavage mechanism).

3.5 Comments on Diverging V-Shaped Cracks

According to observations, diverging V-shaped cracks may also form ahead of an obstacle (e.g., Sanderson 1988, ch. 7); Fig. 4d,e. To estimate in a simple manner a rough approximate value of complementary energy Π^* of an infinite ice plate after formation of such cracks, we may assume that the force P from the structure causes stresses only within the wedge between the cracks (Fig. 4f). From a well-known solution (Timoshenko and Goodier, 1970),

$$\sigma_r = -Pk_\theta \cos\varphi / rh, \qquad \sigma_\varphi = \sigma_{r\varphi} = 0 \tag{45}$$

where σ_r, σ_φ and $\sigma_{r\varphi}$ are the stress components in polar coordinates r, φ, and

$$k_\theta = 1 / (\theta + \tfrac{1}{2}\sin 2\theta) \tag{46}$$

θ being the inclination angle of the cracks (Fig. 4e). The displacement at $r = d/2$ (structure surface) is

$$u = \int_{d/2}^{\infty} \frac{\sigma_r}{E} \mathrm{d}r = \frac{Pk_\theta}{Eh} \ln \frac{2a}{d} \tag{47}$$

Then $\Pi^* = \frac{1}{2}Pu = (P^2 k_\theta / 2Eh) \ln(2a/d)$. The complementary energy before fracture may be estimated as the value of Π^* for $\theta = \pi$, i.e. $\Pi_0^* \approx (P^2/2\pi Eh) \ln(2a/d)$. The total energy release due to V-cracks in the ice plate is $\Delta\Pi^* = \Pi^* - \Pi_0^*$, and the derivative $\partial\Delta\Pi^*/\partial a$ at constant P must be equal to $2hG_f$. This condition yields

$$P \approx 2h \sqrt{\frac{EG_f}{\pi^{-1} - k_\theta}}\, \sqrt{a} \tag{48}$$

To determine crack length a and angle θ, one may use two conditions: 1) the opening displacement at the crack mouth, δ, must be equal to $\chi d/(2\cos\theta)$, which means that the load-point displacement of force P must be $u = (\chi d/2)\tan\theta$, and 2) the expression for P should be minimized with respect to θ. These two conditions, however, make the solution quite complicated. We will not pursue it here because of this, as well as because of two unresolved questions: 1) An axial cleavage crack may be also present, and it may form either before or after the V-cracks. 2) Simultaneous compression crushing is very likely in the case of V-cracks, which makes the value of χ, and thus the lengths a of V-cracks, rather uncertain.

Unlike the cleavage fracture, the V-shaped cracks can occur only from time to time. They do not represent a mechanism that would accommodate continuous movement of the ice.

4 Conclusions

1. The present simplified fracture analysis agrees with previous numerical simulations base on cohesive fracture mechanics and confirms the presence of a strong size effect (effect of ice thickness) on the nominal strength of floating ice plate subjected to a vertical load. The size effect roughly follows the size effect law proposed in 1984 by Bažant. The analysis is instructive in clarifying the fracture mechanism.

2. Simplified fracture analysis of the nominal strength of ice plate pushed against a fixed structure brings to light several mechanisms causing the effects of ice thickness, the diameter of the structure and, if the size of the ice floe is finite, the size of the floe. Buckling of the floating plate causes a reverse size effect of ice thickness (i.e., the nominal strength increasing with ice thickness) and therefore plays any role only for sufficiently thin ice. Cleavage of ice plate against the direction of ice movement causes a size effect of structure diameter which follows linear elastic fracture mechanics (LEFM) for small enough diameters and becomes progressively weaker with increasing diameter. Compression fracture, with ice crushing localized into transversely propagating bands, causes a size effect of ice thickness that follows approximately the classical size effect law proposed in 1984 by Bažant. The overall fracture of a finite ice floe causes a size effect of the floe size, following again the same size effect law.

3. The present approach contrasts with the classical approach based on material strength or plasticity theories, which leads to no size effect.

References

Barenblatt, G.I. (1979). *Similarity, self-similarity and intermediate asymptotics*, Consultants Bureau (Plenum Press), New York, N.Y. (transl. from Russian original, 1978).

Barenblatt, G.I. (1987). *Dimensional analysis*. Gordon and Breach, New York.

Bažant, Z.P. 1984. Size effect in blunt fracture: concrete, rock, and metal . *J. of Engrg. Mech. ASCE*, 110, 518–535.

Bažant, Z.P. 1985. Fracture mechanics and strain-softening in concrete. Preprints, *U.S.-Japan Seminar on Finite Element Analysis of Reinforced Concrete Structures*, Tokyo, Vol. 1, 47–69.

Bažant, Z.P. (1992). "Large-scale thermal bending fracture of sea ice plates." *J. of Geophysical Research*, 97 (C11), 17,739–17,751.

Bažant, Z.P. (1992). "Large-scale fracture of sea ice plates." (Proc. *11th IAHR Ice Symposium*, Banff, Alberta), June (ed. by T.M. Hrudey, Dept. of Civil Engineering, University of Alberta, Edmonton), vol 2., pp. 991–1005.

Bažant, Z.P., 1993, "Scaling laws in mechanics of failure." *J. Engrg. Mech. ASME*, 119 (9) , 1828–1844.

Bažant, Z.P. 1997a. Scaling of quasibrittle fracture: asymptotic analysis. *Int. J. of Fracture*, 83 (1), 19–40.

Bažant, Z.P. 1997. Scaling of quasibrittle fracture: Hypotheses of invasive and lacunar fractality, their critique and Weibull connection. *Int. J. of Fracture* 83 (1), 41–65.

Bažant, Z.P. (1999). "Size effect on structural strength: a review." *Archives of Applied Mechanics* (Ingenieur-Archiv, Springer Verlag) 69, 703–725.

Bažant, Z.P., and Cedolin, L. (1991). *Stability of structures: Elastic, inelastic, fracture and damage theories*, Oxford University Press, New York.

Bažant, Z.P., & Chen, E.-P. (1997). Scaling of structural failure. *Applied Mechanics Reviews* ASME 50 (10), 593–627.

Bažant, Z.P., & Gettu, R. (1991). Size effects in the fracture of quasi-brittle materials. in *Cold Regions Engineering* (Proc., *6th ASCE International Specialty Conference*, held in Hanover, NH, Feb. 1991), D.S. Sodhi (ed.), ASCE, New York, 595–604.

Bažant, Z.P., & Kim, J.-K. (1985). Fracture theory for nonhomogeneous brittle materials with application to ice. Proc. *ASCE Nat. Conf. on Civil Engineering in the Arctic Offshore — ARCTIC 85*, San Francisco, L. F. Bennett (ed.), ASCE, New York, 917–930.

Bažant, Z.P., and Kim, Jang-Jay H. (1998). "Size effect in penetration of sea ice plate with part-through cracks. I. Theory." *J. of Engrg. Mechanics* ASCE 124 (12), 1310–1315; with discussions and closure in Vol. 126 (4), 438–442, 2000.

Bažant, Z.P., and Kim, Jang-Jay H. (1998). "Size effect in penetration of sea ice plate with part-through cracks. II. Results." *J. of Engrg. Mechanics* ASCE 124 (12), 1316–1324; with discussions and closure in Vol. 126 (4), 438–442, 2000.

Bažant, Z.P., Kim, J.J., & Li, Y.-N. 1995. Part-through bending cracks in sea ice plates: Mathematical modeling. *ICE MECHANICS–1995*, J.P. Dempsey & Y. Rajapakse (eds.), ASME AMD-Vol. 207, 97–105.

Bažant, Z.P., and Li, Y.-N. (1994). "Penetration fracture of sea ice plate: Simplified analysis and size effect." *J. of Engrg. Mech.* ASCE 120 (6), 1304–1321.

Bažant, Z.P., and Li, Y.-N. (1995). "Penetration fracture of sea ice plate." *Int. J. Solids Structures* 32, No. 3/4, 303–313.

Bažant, Z.P., and Planas, J. (1998). *Fracture and size effect in concrete and other quasibrittle materials*. CRC, Boca Raton, Florida.

Bažant, Z.P., and Xiang, Yuyin (1997). "Size effect in compression fracture: splitting crack band propagation." *J. of Engrg. Mechanics* ASCE 123 (2), 162–172.

Bernstein, S. 1929. The railway ice crossing (in Russian), *Trudy Nauchno-Technicheskogo Komiteta Narodnogo Komissariata Putei*, Soobshchenniya, Vol. 84, Moscow.

Butiagin, I.P. (1966). *Strength of ice and ice cover*, Izdatel'stvo Nauka, Sibirskoe Otdelenie, Novosibirsk, Russia (154 pp.).

Dempsey, J.P. (1991). "The fracture toughness of ice." *Ice Structure Interaction*, S.J. Jones, R.F. McKenna, J. Tilotson and I.J. Jordaan, Eds., Springer-Verlag, Berlin, 109–145.

Dempsey, P.P. (2000). "Discussion of "Size effect in penetration of ice plate with part-through cracks. I. Theory, II. Results." by Z.P. Bažant and J.J.H. Kim, *J. of Engrg. Mech.* 126 (4), p. 438.

Dempsey, J.P., Adamson, R.M., and Mulmule, S.V., 1995, "Large-scale in-situ fracture of ice." *Proceedings of FRAMCOS-2*, edited by Wittmann, F.H., AEDIFICATIO Publishers, D-79104 Freiburg, 1995.

Dempsey, J.P., Adamson, R.M., and Mulmule, S.V. (1999b). "Scale effects on the *in situ* tensile strength and fracture of ice: Part II.: First-year sea ice at Resolute, N.W.T.". *Int. J. of Fracture 95*, 346–378.

Dempsey, J.P., DeFranco, S.J., Adamson, R.M., and Mulmule, S.V. (1999a). "Scale effects on the *in situ* tensile strength and fracture of ice: Part I.: Large grained freshwater ice at Spray Lakes Reservoir, Alberta". *Int. J. of Fracture* 95 (1999), 325–345.

Dempsey, J.P., Slepyan, L.I., and Shekhtman, I.I., 1995, "Radial cracking with closure." *Int. J. of Fracture*, 73 (3), 233–261.

DeFranco, S.J., and Dempsey, J.P. (1992). "Nonlinear fracture analysis of saline ice: Size, rate and temperature effects." *Proc. of the 11th IAHR Symposium*, Banff, Alberta, Vol.3, 1420–1435.

DeFranco, S.J., and Dempsey, J.P. (1994). "Crack propagation and fracture resistance in saline ice." *J. Glaciology* 40, 451–462.

DeFranco, S.J., Wei, Y., and Dempsey, J.P. (1991). "Notch acuity effects on fracture of saline ice." *Annals of Glaciology* 15, 230–235.

Fisher, R.A. and Tippett, L.H.C. (1928). "Limiting forms of the frequency distribution of the largest and smallest member of a sample." *Proc., Cambridge Philosophical Society* 24, 180–190.

Frankenstein, E.G., 1963, "Load test data for lake ice sheet." *Technical Report 89*, U.S. Army Cold Regions Research and Engineering Laboratory, Hanover, New Hampshire.

Frankenstein, E.G., 1966, "Strength of ice sheets." *Proc., Conf. on Ice Pressures against Struct.; Tech. Memor. No. 92, NRCC No. 9851*, Laval University, Quebec, National Research Council of Canada, Canada, 79–87.

Li, Y.-N., and Bažant, Z.P. (1994). "Penetration fracture of ice plate: 2D analysis and size effect." *J. of Engrg. Mech.* ASCE 120 (7), 1481–1498.

Li, Zhengzhi, and Bažant, Z.P. (1998). "Acoustic emissions in fracturing sea ice plate

simulated by particle system." *J. of Engrg. Mechanics* ASCE 124 (1), 69–79.
Kittl, P. and Diaz, G. (1988). "Weibull's fracture statistics, or probabilistic strength of materials: state of the art." *Res Mechanica*, 24, 99-207.
Lichtenberger, G.J., Jones, J.W., Stegall, R.D., and Zadow, D.W., 1974, "Static ice loading tests Resolute Bay – Winter 1973/74." *APOA Proj. No. 64, Rep. No. 745B-74-14, (CREEL Bib # 34-3095)*, Sunoco Sci. & Technol., Rechardson, Tex.
Kerr, A.D., 1975, "The bearing capacity of floating ice plates subjected to static or quasi-static loads – A critical survey." *Research Report 333*, U.S. Army Cold Regions Research and Engineering Laboratory, Hanover, New Hampshire.
Kerr, A.D., 1996, "Bearing capacity of floating ice covers subjected to static, moving, and oscillatory loads." *Appl. Mech. Rev., ASME Reprint*, 49 (11), 463–476.
Mariotte, E. (1686). *Traité du mouvement des eaux*, posthumously edited by M. de la Hire; Engl. transl. by J.T. Desvaguliers, London (1718), p. 249; also *Mariotte's collected works*, 2nd ed., The Hague (1740).
Mulmule, S.V., Dempsey, J.P., and Adamson, R.M., 1995, "Large-scale in-situ ice fracture experiments - part II: modeling efforts, in ice mechanics - 1995 ." ASME Joint Applied Mechanics and Materials Summer Conference, AMD - MD 1995, University of California, Loas Angeles, June 28-30, 1995.
Murakami, Y., ed. (1987). Stress Intensity Factors Handbook, Pergamon Press, Oxford and New York, Vol. 1.
Nevel, D.E., 1958, "The theory of narrow infinite wedge on an elastic foundation," *Transactions, Engineering Institute of Canada*, 2(3)
Peirce, F.T. (1926). *J. Textile Inst.*, 17, 355.
Rice, J.R. and Levy, N. (1972). "The part-through surface crack in an elastic plate." *J. Appl. Mech. ASME*, 39, 185–194.
Sanderson, T.J.O. (1988). *Ice Mechanics: Risks to Offshore Structures*, Graham and Trotman Limited, London.
Schulson, E.M. (1990). "The brittle compressive fracture of ice." *Acta Metall. Mater.* 38 (10), 1963-1976.
Schulson, E.M. (2000). "Brittle failure of ice." *Engineering Fracture Mechanics*, in press.
Sedov, L.I. (1959). *Similarity and dimensional methods in mechanics.* Academic Press, New York.
Slepyan, L.I. (1990). "Modeling of fracture of sheet ice." *Mechanics of Solids* (transl. of Izv. AN SSSR Mekhanika Tverdoga Tela), 155–161.
Sodhi, D.S. (1995a). "Breakthrough loads of floating ice sheets." *J. Cold Regions Engrg. ASCE*, 9 (1), 4–20.
Sodhi, D.S. (1995b). "Wedging action during vertical penetration of floating ice sheets." *AMD-Vol.207, Ice Mechanics*, Book No. H00954, 1995, 65–80.
Sodhi, D.S. (1996). "Deflection analysis of radially cracked floating ice sheets." *17th Int. Conf. OMAE Proceedings*, Book No. G00954, 1996, 97–101.
Sodhi, D.S. (1998). "Vertical penetration of floating ice sheets." *Int. J. of Solids and Structures* 35 (31–32), 4275–4294.
Sodhi, D.S. (2000). "Discussion of "Size effect in penetration of ice plate with part-through cracks. I. Theory, II. Results." by Z.P. Bažant and J.J.H. Kim, *J. of Engrg. Mech.* 126 (4), 438–440.
Tada, H., Paris, P.C., and Irwin, J.K. (1985). *The Stress Analysis of Cracks Handbook*, 2nd ed., Paris Productions, Inc., St. Louis, MO.
Timoshenko, S.P., and Goodier, J.N. (1970). *Theory of elasticity.* 3rd ed., McGraw Hill, New York (p. 110).
Weeks, W.F., & Mellor, M. (1984). "Mechanical properties of ice in the Arctic seas". *Arctic Technology & Policy*, I. Dyer & C. Chryssostomidis (eds.), Hemisphere, Washington, D.C., 235-259.
Weeks, W.F., and Assur, A. (1972). "Fracture of lake and sea ice." *Fracture*, H. Liebowitz, Ed., Vol. II, 879–978.
Weibull, W. (1939). "The phenomenon of rupture in solids." Proc., Royal Swedish Institute of Engineering Research (Ingenioersvetenskaps Akad. Handl.) 153, Stockholm, 1–55.